Nrl is required for rod photoreceptor development

Alan J. Mears[1], Mineo Kondo[1,2], Prabodha K. Swain[1], Yuichiro Takada[1], Ronald A. Bush[1], Thomas L. Saunders[3], Paul A. Sieving[1,4] & Anand Swaroop[1,3]

Published online: 5 November 2001, DOI: 10.1038/ng774

The protein neural retina leucine zipper (Nrl) is a basic motif–leucine zipper transcription factor that is preferentially expressed in rod photoreceptors[1,2]. It acts synergistically with Crx to regulate rhodopsin transcription[3–5]. Missense mutations in human *NRL* have been associated with autosomal dominant retinitis pigmentosa[6,7]. Here we report that deletion of *Nrl* in mice results in the complete loss of rod function and super-normal cone function, mediated by S cones. The photoreceptors in the *Nrl*$^{-/-}$ retina have cone-like nuclear morphology[8] and short, sparse outer segments with abnormal disks. Analysis of retinal gene expression confirms the apparent functional transformation of rods into S cones in the *Nrl*$^{-/-}$ retina. On the basis of these findings, we postulate that *Nrl* acts as a 'molecular switch' during rod-cell development by directly modulating rod-specific genes while simultaneously inhibiting the S-cone pathway through the activation of *Nr2e3*.

We deleted the entire coding region (exons 2 and 3) of *Nrl* by homologous recombination (Fig. 1*a*) and confirmed the deletion by Southern blot and PCR analysis (Fig. 1*b*,*c*). The *Nrl*$^{+/-}$ and *Nrl*$^{-/-}$ mice were morphologically normal, viable and fertile. We confirmed the loss of the Nrl protein and mRNA by immunoblot analysis (Fig. 1*d*) and RT–PCR (Fig. 1*e*).

To evaluate retinal function *in vivo*, we recorded electroretinograms (ERGs) with various stimulus intensities under dark- and light-adapted conditions from wildtype, *Nrl*$^{+/-}$ and *Nrl*$^{-/-}$ mice. ERG intensity series obtained from dark-adapted *Nrl*$^{+/-}$ mice were similar to those of wildtype mice (Fig. 2*a*,*b*). In contrast, there was a complete absence of rod function in *Nrl*$^{-/-}$ mice. In light-adapted conditions, the b-wave threshold was the same for wildtype and *Nrl*$^{-/-}$ mice, indicating a functional cone pathway in *Nrl*$^{-/-}$ retina (Fig. 2*c*,*d*). The amplitude of the maximum light-adapted ERG b-wave for the *Nrl*$^{-/-}$ mice was two to three times larger than that for the wildtype mice, however, indicating enhanced cone-mediated activity (Fig. 2*c*). To determine if S or M cones mediate the large

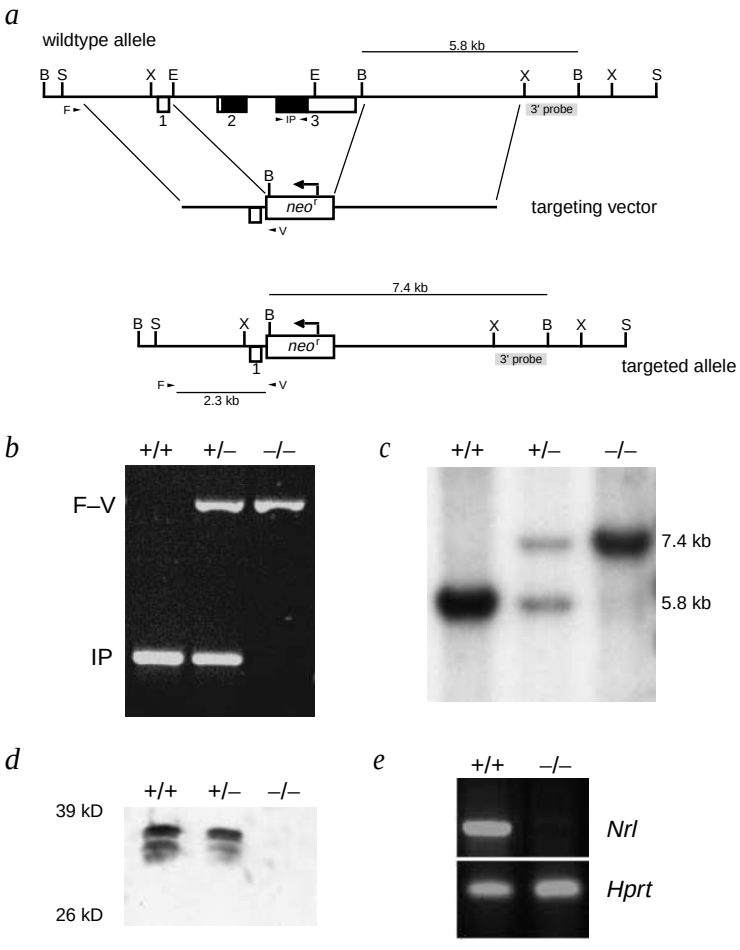

Fig. 1 Targeted disruption of *Nrl* in mouse. ***a***, Strategy for targeting *Nrl*. Wildtype locus is shown at top. Open boxes indicate exons (1–3); filled boxes, the coding region. Small arrowheads represent the primers used for the 5′ screen (F and V). The 1.4-kb 3′ probe (*Xho*I–*Bam*HI fragment) detects a 5.8-kb *Bam*HI fragment in wildtype genomic DNA. The targeting vector was constructed with 2.2 kb of 5′ flanking sequence and 4.4 kb of 3′ flanking sequence. Exons 2 and 3 include the entire coding sequence of *Nrl* and are replaced with the PGK-*neo*^{r} cassette. Targeted events were identified by the presence of the 5′ F–V 2.3-kb product and the 7.4-kb *Bam*HI fragment as detected by the 3′ probe. IP, internal control PCR product; B, *Bam*HI; E, *Eco*RI; S, *Sal*I; X, *Xho*I. ***b***, PCR analysis of mouse-tail genomic DNA. The 2.3-kb F–V junction PCR product is detected only in *Nrl*$^{+/-}$ and *Nrl*$^{-/-}$ mice. The 607-bp internal PCR product (IP) of exon 3 is detected only in the wildtype and *Nrl*$^{+/-}$ mice. ***c***, Southern blot of *Bam*HI-digested mouse-tail genomic DNA. The external 3′ probe detects a 5.8-kb fragment corresponding to the wildtype allele and a 7.4-kb fragment corresponding to the targeted allele. ***d***, Immunoblot of protein extracts from mouse retina (P10). The antibody pAb-Nrl detects several different isoforms of Nrl in the 29–35-kD range, all of which are absent in *Nrl*$^{-/-}$ mice. ***e***, RT–PCR of retinal RNA isolated from P10 mice. *Nrl* primers were from exons 2 and 3, amplifying a 540-bp product. *Hprt* primers were used as a control (151 bp).

[1]*Department of Ophthalmology and Visual Sciences, University of Michigan, Ann Arbor, Michigan 48105, USA.* [2]*Department of Ophthalmology, Nagoya University School of Medicine, Nagoya, Japan 466-8550.* [3]*Department of Human Genetics, University of Michigan, Ann Arbor, Michigan, USA.* [4]*National Eye Institute, National Institutes of Health, Bethesda, Maryland, USA. Correspondence should be addressed to A.S. (e-mail: swaroop@umich.edu).*

light-adapted responses, we recorded ERGs with monochromatic stimuli of 400 nm or 530 nm. The amplitude of the S cone–mediated response (400 nm) was more than six times larger for the $Nrl^{-/-}$ mice than for the wild type (Fig. 2*e*), whereas the M-cone response was not significantly altered, suggesting a super-normal S-cone function similar to the clinical phenotype of enhanced S-cone syndrome (ESCS) in humans[9].

To examine the effect of age on retinal function, we recorded ERGs of $Nrl^{-/-}$ mice at different times after birth (Fig. 2*f*). The amplitude of light-adapted ERG responses elicited by maximum stimulus did not change significantly up to 31 weeks, suggesting that cones can survive without rod function.

Light microscopy of retinae from 5-wk wildtype, $Nrl^{+/-}$ and $Nrl^{-/-}$ mice indicated that the outer nuclear layer (ONL) of the $Nrl^{-/-}$ retina had a similar thickness and number of nuclei as the wild type; however, it was disrupted with whorls and rosettes (Fig. 3*a–c*). A majority of photoreceptor nuclei in the $Nrl^{-/-}$ retina were ellipsoid and showed a distributed pattern of heterochromatin, characteristic of cones[8]. By 31 weeks, the rosettes and whorls were no longer evident and concomitant thinning of the ONL had occurred (data not shown), a phenotypic pattern reminiscent of that in *rd7* mice[10]. The retinae of $Nrl^{+/-}$ mice appear normal.

Ultrastructural analysis of the $Nrl^{-/-}$ retina shows considerably fewer (approximately 20% of normal) and noticeably shorter outer segments with abnormal disk morphology (Fig. 3*d–h*). In contrast to the lamellar array of outer segment disks observed in the wild type, the outer segment disks of the $Nrl^{-/-}$ retinae were often misaligned and abnormally associated with the retinal pigment epithelium (RPE).

Immunohistochemical analysis of retinae from 5-wk mice shows a similar distribution of rhodopsin, S-opsin and M-opsin in wildtype and $Nrl^{+/-}$ mice. In the $Nrl^{-/-}$ retina, M-opsin distribution seemed to be normal, but we detected no rhodopsin immunoreactivity and observed S-opsin throughout the outer segments (Fig. 4). These findings are consistent with the ERG data, showing a loss of rod and 'gain' of S- but not M-cone activity.

We analyzed retinal gene expression at post-natal day (P) 10, an age prior to eye opening and formation of the outer segments when the phototransduction genes are highly expressed[11]. Northern blot and immunoblot analyses of $Nrl^{-/-}$ retinae indicate significant changes in the expression profile (Fig. 5). We detected no expression of the rod-specific genes encoding rhodopsin (*Rho*), rod transducin (*Gnat1*) or the cGMP phosphodiesterase β subunit (*Pdeb*), whereas the expression of cone genes encoding S-opsin (*Opn1sw*), cone transducin (*Gnat2*) and cone arrestin was dramatically increased. Consistent with ERG and immunohistochemistry, M-opsin expression was unaltered. Expression of the genes encoding rod arrestin (*Sag*), *Rom1*, *Abca4*, *Rp1h* and *Rcvrn* (genes expressed in both rod and cone photoreceptors) is reduced by 40–70% in $Nrl^{-/-}$ retina. Semi-quantitative RT–PCR results are consistent with northern blot analysis (data not shown).

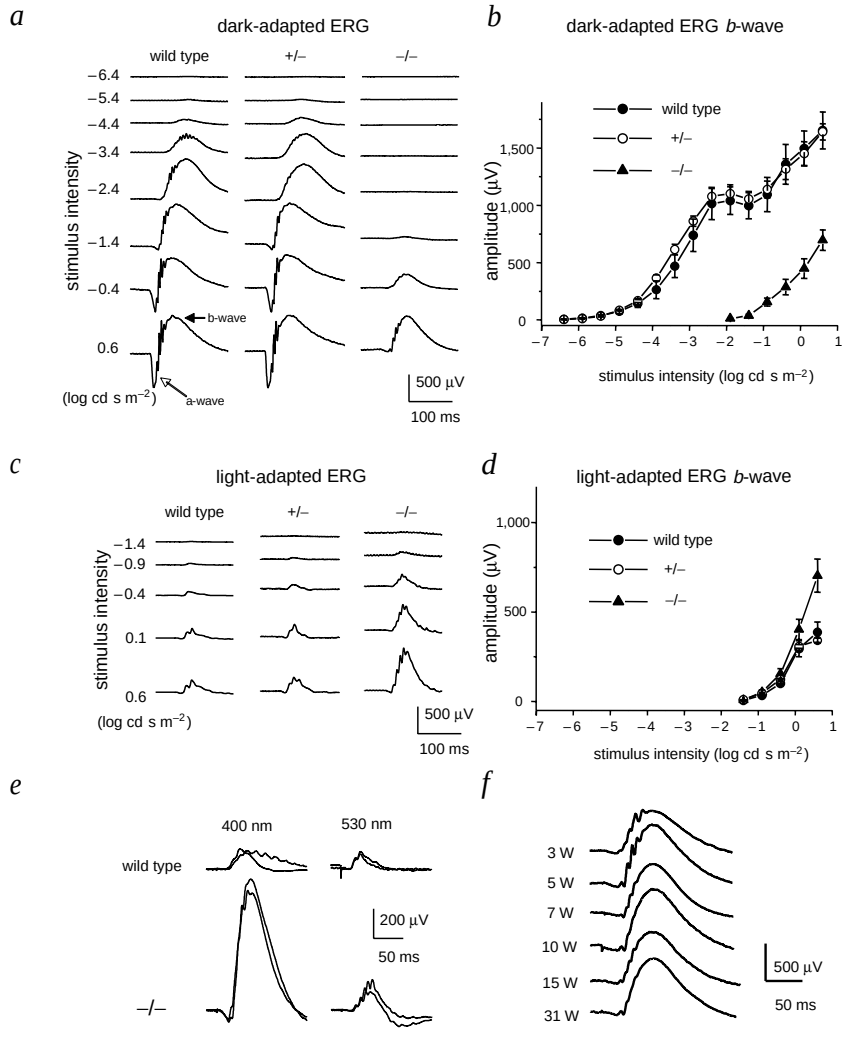

Fig. 2 Electroretinography. ***a***, Dark-adapted flash ERG responses from 5-wk wildtype, $Nrl^{+/-}$ and $Nrl^{-/-}$ mice, recorded in a Ganzfeld bowl. The ERG response at high stimulus intensities (–0.4 log cd s m^{-2} and higher) in the $Nrl^{-/-}$ mouse represents cone function[30]. ***b***, Intensity-response curves of the dark-adapted ERG *b*-wave for three wildtype, $Nrl^{+/-}$ and $Nrl^{-/-}$ mice. Mean and s.e.m. are indicated. ***c***, Light-adapted ERG responses from 5-wk wildtype, $Nrl^{+/-}$ and $Nrl^{-/-}$ mice. ***d***, Intensity–response curves of the light-adapted ERGs for three wildtype, $Nrl^{+/-}$ and $Nrl^{-/-}$ mice. Mean and s.e.m. are indicated. ***e***, Light-adapted ERG responses to photopically balanced stimuli at two wavelengths. Monochromatic stimuli at 400 nm and 530 nm (10-nm half-bandwidth interference filter) were matched to produce approximately equal response amplitude for wildtype mice. $Nrl^{-/-}$ mice show a severe mismatch, with considerably larger responses to the short-wavelength stimulus. Results from two different animals are superimposed. ***f***, ERG responses serially recorded from $Nrl^{-/-}$ mice at 3, 5, 7, 10, 15 and 31 wk. Dark-adapted ERGs were recorded with a stimulus intensity of 0.6 log cd s m^{-2}. Response amplitude did not change significantly with age up to 31 wk.

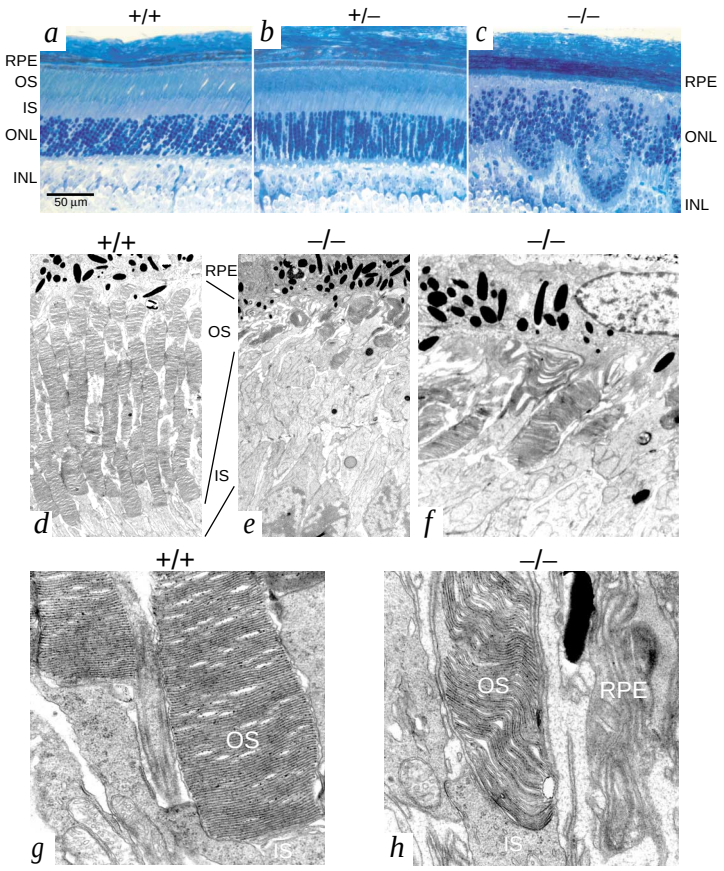

Fig. 3 Light microscopy and ultrastructural analysis of retina. ***a***,***b***,***c***, Retinal sections from 5-wk wildtype, *Nrl*$^{+/-}$ and *Nrl*$^{-/-}$ mice counterstained with toluidine blue. *Nrl*$^{+/-}$ retina appears normal; *Nrl*$^{-/-}$ retina is grossly abnormal. The photoreceptor nuclei (ONL) show a dispersed pattern of heterochromatin characteristic of cone nuclei. The ONL is disrupted by rosette-like structures of photoreceptors. In addition, the inner segment and outer segment layers are barely discernible and considerably shorter. RPE, retinal pigment epithelium; IS, inner segment; OS, outer segment; ONL, outer nuclear layer; INL, inner nuclear layer. ***d***,***e***, Electron micrographs of wildtype and *Nrl*$^{-/-}$ retina (magnification ×1,950). Outer segments are sparse and considerably shorter in the *Nrl*$^{-/-}$ retina. ***f***, *Nrl*$^{-/-}$ retina showing some photoreceptors with relatively normal packing of disks and others with considerable disorganization (magnification ×4,600). ***g***,***h***, Outer segments of wildtype retina and *Nrl*$^{-/-}$ retina (magnification ×25,000).

Phenotypic similarities between ESCS and the *Nrl*$^{-/-}$ mice prompted us to examine *Nr2e3* expression. No *Nr2e3* transcripts were detected in the *Nrl*$^{-/-}$ retina by northern blot (Fig. 5) and RT–PCR analysis (data not shown). Our results are consistent with previous studies[10,12,13] reporting *Nr2e3* expression specifically in photoreceptors and suggest that Nrl is upstream of Nr2e3 in the photoreceptor-development hierarchy. The detection of *Nrl* transcripts before those of *Nr2e3*, at embryonic day (E) 16.5–18.5 compared with E18.5–P0.5 (ref. 13), in developing mouse retina supports this assertion (data not shown). We detected no significant changes in protein levels for Prkca (protein kinase C-α, a rod bipolar cell marker)[14], Rlbp1 (expressed in Müller glial cells and retinal pigment epithelium)[15] and rhodopsin kinase (expressed in rods and cones)[16]. The protein Gfap (glial fibrillary acidic protein, a marker for retinal astrocytes and stressed Müller cells)[17] is increased in the *Nrl*$^{-/-}$ retina, reminiscent of its enhanced expression under conditions of retinal stress and degeneration[18].

Functional switching of photoreceptors from a rod to an S-cone phenotype in the *Nrl*$^{-/-}$ retina is evident from the change both in ERG and in the expression of the components of the phototransduction cascade. Although the *Nrl*$^{-/-}$ mouse is functionally rodless, the structural changes do not indicate a 'true' transformation of rods to cones. The outer segments of the photoreceptors are sparse, appear anatomically abnormal and are not appropriately arranged in organized lamellar arrays. We propose that these photoreceptors may be cone–rod intermediates (or 'cods') that function as cones but may not elaborate the full differentiation program. The abnormal disk organization of these photoreceptors may be due to the collapse of subretinal space caused by the lack of rods (which are densely packed and have

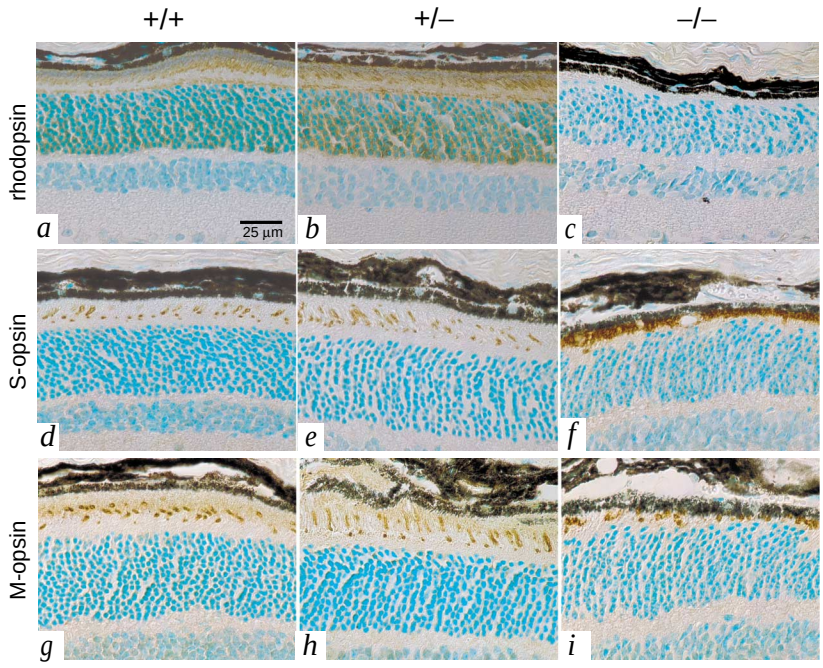

Fig. 4 Opsin immunohistochemistry. Immunostaining of retinal sections from 5-wk wildtype, *Nrl*$^{+/-}$ and *Nrl*$^{-/-}$ mice with antibodies. ***a***,***b***, Wildtype and *Nrl*$^{+/-}$ retinae show a normal distribution of rhodopsin antibody (indicated by light brown color). ***c***, Rhodopsin is absent in the shortened outer segment layer of the *Nrl*$^{-/-}$ retina. ***d***,***e***, Wildtype and *Nrl*$^{+/-}$ retinae show normal distribution of S-opsin antibody. ***f***, *Nrl*$^{-/-}$ retina shows S-opsin staining of the entire outer segment layer. ***g***,***h***,***i***, M-opsin antibody shows normal distribution in all retinae.

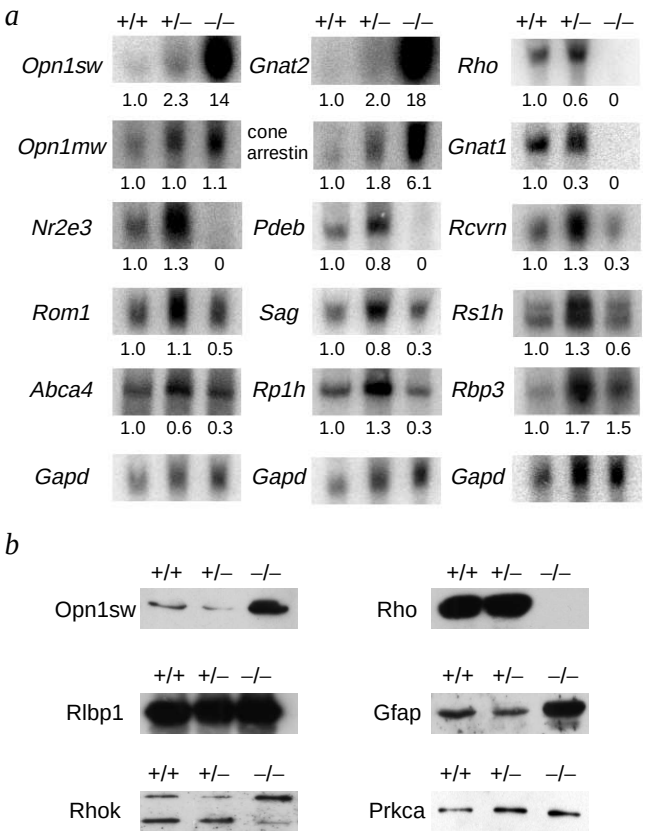

Fig. 5 Expression analysis of P10 mouse retina. ***a***, Each column represents a different northern blot of RNA isolated from P10 wildtype, *Nrl*$^{+/-}$ and *Nrl*$^{-/-}$ retinae. Each blot was hybridized to *Gapd* to normalize for loading differences. Ratios of amounts of RNA were as follows: left and middle columns, 1.0:2.1:2.5; right column, 1.0:1.9:1.7. Signals from cDNAs were normalized to *Gapd* and expression ratios calculated relative to that of the wild type (ratios are shown for each cDNA probe below each panel). Radiolabeled mouse cDNA probes are designated according to the gene from which they were derived, which encode components of the phototransduction cascade—blue cone opsin (*Opn1sw*), green cone opsin (*Opn1mw*), rod transducin (*Gnat1*), cone transducin (*Gnat2*), cone arrestin, rod arrestin (*Sag*), recoverin (*Rcvrn*) and phosphodiesterase β subunit (*Pdeb*). Rod outer segment membrane protein 1 (*Rom1*) is a structural component of outer segment disks. The ATP-binding cassette transporter (*Abca4*) is thought to be involved in the transport of all-*trans* retinal and retinal across outer segment membranes. Interphotoreceptor retinol-binding protein (*Rbp3*) is believed to transport retinoids between the retinal pigment epithelium and the photoreceptors. Retinoschisin (*Rs1h*) is expressed in photoreceptors and bipolar cells and is thought to be involved in cell adhesion. The *Rp1h* gene product may have a role either in the trafficking of phototransductive proteins from the inner segment to the outer segment or in the maintenance of the structure of the connecting cilium. ***b***, Immunoblots of P10 wildtype, *Nrl*$^{+/-}$ and *Nrl*$^{-/-}$ retinal proteins. Equal amounts of retinal protein (50 μg) were loaded in each lane. In the *Nrl*$^{-/-}$ mouse, the amount of S-opsin (Opn1sw) protein is greatly increased, but there is no detectable rhodopsin (Rho). Rhodopsin kinase (Rhok), which is expressed in rods and cones, shows no alteration in absolute protein levels; however, the two bands, representing different isoforms of this protein, do show a change in relative levels in the wildtype and *Nrl*$^{-/-}$ mice. Cellular retinaldehyde-binding protein (Rlbp1), which is expressed in retinal pigment epithelium and Müller cells, shows no change in protein levels. Glial fibrillary acidic protein (Gfap), which is expressed in Müller cells, is upregulated in the *Nrl*$^{-/-}$ retina. Protein kinase C-α (Prkca), which is expressed in the glial, rod bipolar and some amacrine cells, is unaltered in the *Nrl*$^{-/-}$ retina.

large outer segments) or to Nrl's regulation (direct or indirect) of cytoskeletal components necessary for maintaining photoreceptor structure and morphology[19].

The ability of retinal progenitor cells (RPCs) to follow a precise developmental pathway is regulated by a limited number of transcription factors before and during photoreceptor differentiation[20–23]. The RPCs may go through a sequential order of competence states in which the ability to assume particular cell fates is acquired and lost over developmental time[22]. With respect to photoreceptor cell fates, the competence model proposes that the cones are generated first from RPCs and then the remaining progenitors pass through additional competence states before giving rise to rods[20,21]. Based on our current data and previously proposed schemes[20–23], we postulate a modified competence model (Fig. 6), in which Nrl plays a pivotal role in the determination of photoreceptor phenotype.

Methods

Production of gene-targeted mice. We isolated mouse *Nrl* genomic clones from a 129X1/SvJ-derived Lambda Fix II genomic library (Stratagene) and partially sequenced them. To construct the targeting vector, we cloned the 5′ genomic flanking sequence (2.1 kb) into *Eco*RI site and cloned the 3′ flanking sequence (4.4 kb) into *Xho*I site of the pPNT vector[24] (gift of R. Mulligan). The targeting vector was linearized with *Not*I and electroporated into R1 embryonic stem (ES) cells[25]. PCR amplification of ES clone DNA with a 5′ flanking primer (5′–TTTGTCCCAGTGATAAGGTGAG–3′) and a vector-specific primer (5′–GTTCTAATTCCATCAGAAGCTGAC–3′) detected a 2.3-kb product in targeted alleles. For PCR genotyping purposes, we detected the wildtype allele by amplification of a 607-bp fragment of *Nrl* exon 3 (forward primer, 5′–GCTGGTCTCGATGTCTGT–3′; reverse, 5′–CATTCAGCATGCCACCTG–3′). We injected targeted ES clones into C57BL/6J blastocysts to generate ES cell–mouse chimeras, which were mated to C57BL/6J females to transmit the targeted allele[26].

ERG recordings. We prepared animals in dim red light and anesthetized them with xylazine (13 mg per kg by intramuscular injection) and ketamine (86 mg per kg intramuscular). Pupils were dilated with 0.1% atropine and 0.1% phenylephrine HCl. Body temperature was maintained near 38 °C with a heating pad. We recorded ERGs with gold-wire corneal loops under 1% tetracaine topical anesthesia and 3% methylcellulose. We placed gold-wire differential electrodes on the sclera near the limbus, attached a ground wire to the ear and amplified responses (10,000 gain, 0.1–1,000 Hz). We presented xenon photostrobe full-field 30-μs flashes (Grass, PS-22) in a Ganzfeld bowl, with maximum intensity of 0.6 log cd s m^{-2}. Stimulus intensity was attenuated with neutral density filters. We elicited photopic cone ERGs with 0.6 log cd s m^{-2} maximum intensity flashes on a rod-suppressing 43 cd m^{-2} white background. We evaluated responses of S and M cones in wildtype mice using 1-ms photostrobe flashes (Vivitar 238) that were limited to 400 nm or 540 nm using narrow-band interference filters (nominal half-bandwidth of 10 nm). We adjusted strobe intensity to give equal amplitude responses for both wavelengths and then used these stimuli to assess relative S-cone versus M-cone responses in *Nrl*$^{-/-}$ mice.

Histology. We dissected mouse eyes, removing the cornea and lens and leaving half eyecups. We carried out initial fixation with either 4% cacodylate-buffered glutaraldehyde or Karnasky's fixative. Tissue was washed twice with 0.1 M cacodylate buffer and then post-fixed for 1 h with 2% cacodylate-buffered OsO_4 (4% OsO_4 and 0.2 M cacodylate, mixed 1:1). After one wash with 0.1 M cacodylate buffer, tissue was dehydrated in a graded alcohol series. We carried out infiltration with mixtures of epon and propylene oxide and then embedded the tissue in pure epon in the bottom of a beam capsule. We carried out sectioning with a Reichert ultramicrotome and stained sections with toluidine blue.

Transmission electron microscopy. We prepared retinal tissues from 5-wk mice as previously described[27]. We collected sections (80–90 nm) on Formvar-coated 100-mesh copper grids. We obtained images using a Philips CM100 electron microscope at 60 kV.

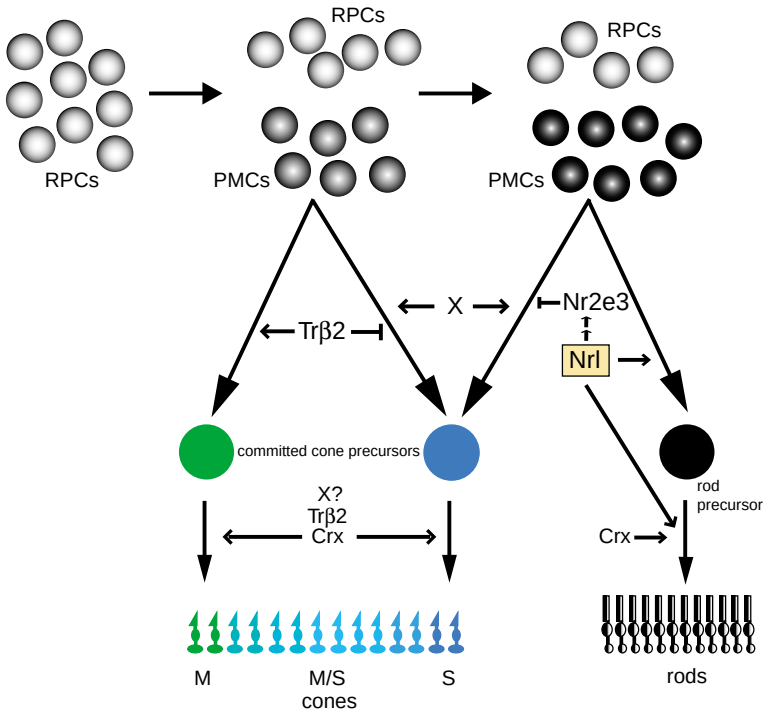

Fig. 6 A model of photoreceptor differentiation in mice. Retinal progenitor cells (RPCs) pass through different stages of competence during development. Post-mitotic cells (PMCs) commit to a particular cone or rod fate in response to a combinatorial action of extrinsic stimuli and transcription factors. Initially, a pool of multipotent progenitors acquires the competence to become cone photoreceptors. In response to thyroid hormone receptor β2 (Trβ2), some commit to the M-cone fate[31]. The lack of Trβ2 and/or the presence of an unidentified factor X direct cone progenitors down the S-cone pathway. Relative response to Trβ2, the factor X and Crx probably modulates differential expression of the two cone opsin pigments. Later in development and in response to extrinsic factors, another pool of post-mitotic RPCs acquires competence to an S-cone or a rod-cell fate (but not the M-cone fate). The expression of Nrl forces these cells to become rod precursors. Working alone or in concert with other transcription factors such as Crx, Nrl directly activates the expression of several genes that encode rod-specific phototransduction proteins, including rhodopsin, Pdeb and rod transducin. Nrl may directly or indirectly regulate the expression of *Nr2e3*, which suppresses the S-cone pathway[9,13], finalizing the commitment to becoming a rod.

Immunohistochemistry. We fixed eyes in 20% neutral buffered formalin at room temperature (RT) overnight. Samples were dehydrated in isopropyl alcohol, cleared in xylene and embedded in paraffin. We cut sections 4 μm thick (Reichert-Jung cryostat) and mounted them on silanized slides. The sections were deparaffinized in xylene, rehydrated in a series of ethanol and then rinsed in PBS. For antigen retrieval treatment, we incubated the sections in 0.1% trypsin at 37 °C for 30 min. We then incubated them sequentially (i) with an affinity-purified rabbit anti–L/M and S-opsin antibody (JH492 and JH455 respectively; gift of J. Nathans) and a mouse anti-rhodopsin monoclonal antibody (1D4; gift of R. Molday) at 4 °C overnight (ii) with biotinylated goat anti-rabbit IgG (Vector) for L/M and S-opsin or biotinylated rabbit anti-mouse IgG (Vector) for anti-rhodopsin at 4 °C for 1 h and (iii) with streptavidin–biotin complex (sABC) solution (Vector) at room temperature for 1 h. We rinsed the sections in PBS and developed the horseradish peroxidase reaction with diaminobenzidine (DAB). We used methyl green as the counterstain.

RNA isolation. We isolated total RNA from embryonic and post-natal retinal tissues using TRIzol reagent (Life Technologies), following the manufacturer's guidelines. We obtained timed pregnant females (C57BL/6) for embryonic stage retinae from Charles River Laboratories.

RT–PCR analysis of retinal RNA. We carried out oligo-dT–primed reverse-transcription reactions with 2.5 μg of total retinal RNA using SuperScript II (Life Technologies). We then used cDNA as template in PCR reactions; *Nrl* was amplified with an exon 2 forward primer (5′–CTATGG AAGGGCCTCTTGG–3′) and an exon 3 reverse primer (5′–GCCACGATG CTCAGAAGTTT–3′), yielding a 540-bp product. We used *Hprt* as an internal standard for the reactions and amplified a 151-bp product with an exon 6 forward primer (5′–CAAACTTTGCTTTCCCTGGT–3′) and an exon 8 reverse primer (5′–CAAGGGCATATCCAACAACA–3′).

Northern blot analysis. We carried out electrophoresis and transfer of RNA following standard protocols[28] using Hybond XL membrane (Amersham). We amplified cDNA probes for all tested genes by RT–PCR from wildtype mouse–retinal RNA. The probes were sequence-verified and labeled with [α^{32}P]dCTP using the Rediprime II random-prime labeling system (Amersham). We carried out hybridizations with ExpressHyb solution (Clontech) using the manufacturer's guidelines. We quantified band signal intensities using the Storm 840 Imaging System (Amersham).

Immunoblot analysis. Retinae were sonicated in 20 mM Tris buffer, pH 8.0, containing 150 mM NaCl and a cocktail of protease inhibitors (Amersham). We estimated the protein concentration with bicinchoninic acid reagent (Sigma). We solubilized samples (approximately 50 μg each) in 2 × SDS lysis buffer by heating at 100 °C for 5 min and then separated them by SDS–PAGE. We transferred proteins to nitrocellulose membrane by electroblotting and carried out immunoblot analysis according to standard protocols[29]. The source and the dilution of the antibody used for immunoblot analysis are: rhodopsin monoclonal antibody (4D2; gift of R. Molday) at 1:300 dilution, S-opsin polyclonal antibody at 1:15 (gift of M. Applebury), NRL polyclonal antibody at 1:3,000 (ref. 2), Rlbp1 polyclonal antibody (kind gift of J. Saari) at 1:2,000, Prkca monoclonal antibody (MC5; Santa Cruz Biotechnology) at 1:200, Gfap polyclonal antibody (Sigma) and rhodopsin kinase polyclonal antibody (Santa Cruz Biotechnology) at 1:200.

Acknowledgments

We thank M. Akimoto, R. Farjo, P. Gillespie III, M. Gillett, S. Hiriyanna, B. Nelson, D. Sorenson, A. Tumath and M. Van Keuren for technical assistance. We are grateful to T. Glaser, P. Hitchcock and P. Raymond for comments on the manuscript. We acknowledge M. Applebury, R. Molday, J. Nathans and J. Saari for antibodies, C. Cepko, D. Deretic, S.G. Jacobson and D. Williams for constructive discussions and A. Nagy, R. Nagy and W. Abramow-Newerly for providing the R1 ES cells. This research was supported by grants from the National Institutes of Health [EY11115, EY07003], The Foundation Fighting Blindness, and Research to Prevent Blindness (RPB). A.S. is a recipient of a Lew R. Wasserman Merit Award from RPB.

Received 3 July; accepted 28 September 2001.

1. Swaroop, A. *et al.* A conserved retina-specific gene encodes a basic motif/leucine zipper domain. *Proc. Natl Acad. Sci. USA* **89**, 266–270 (1992).
2. Swain, P.K. *et al.* Multiple phosphorylated isoforms of NRL are expressed in rod photoreceptors. *J. Biol. Chem.* **276**, 36824–36830 (2001).
3. Rehemtulla, A. *et al.* The basic motif-leucine zipper transcription factor Nrl can positively regulate rhodopsin gene expression. *Proc. Natl Acad. Sci. USA* **93**, 191–195 (1996).
4. Chen, S. *et al.* Crx, a novel Otx-like paired-homeodomain protein, binds to and transactivates photoreceptor cell-specific genes. *Neuron* **19**, 1017–1030 (1997).
5. Mitton, K.P. *et al.* The leucine zipper of NRL interacts with the CRX homeodomain. A possible mechanism of transcriptional synergy in rhodopsin regulation. *J. Biol. Chem.* **275**, 29794–29799 (2000).
6. Bessant, D.A. *et al.* A mutation in NRL is associated with autosomal dominant retinitis pigmentosa. *Nature Genet.* **21**, 355–356 (1999).
7. Martinez-Gimeno, M. *et al.* Mutations P51L and G122E in retinal transcription factor NRL associated with autosomal dominant and sporadic retinitis pigmentosa. *Hum. Mutat.* **17**, 520 (2001).

8. Carter-Dawson, L.D. & LaVail, M.M. Rods and cones in the mouse retina I. Structural analysis using light and electron microscopy. *J. Comp. Neurol.* **188**, 245–262 (1979).
9. Haider, N.B. *et al*. Mutation of a nuclear receptor gene, NR2E3, causes enhanced S cone syndrome, a disorder of retinal cell fate. *Nature Genet.* **24**, 127–131 (2000).
10. Akhmedov, N.B. *et al*. A deletion in a photoreceptor-specific nuclear receptor mRNA causes retinal degeneration in the *rd7* mouse. *Proc. Natl Acad. Sci. USA* **97**, 5551–5556 (2000).
11. Furukawa, T., Morrow, E.M., Li, T., Davis, F.C. & Cepko, C.L. Retinopathy and attenuated circadian entrainment in *Crx*-deficient mice. *Nature Genet.* **23**, 466–470 (1999).
12. Kobayashi, M. *et al*. Identification of a photoreceptor cell–specific nuclear receptor. *Proc. Natl Acad. Sci. USA* **96**, 4814–4819 (1999).
13. Haider, N.B., Naggert, J.K. & Nishina, P.M. Excess cone cell proliferation due to lack of a functional NR2E3 causes retinal dysplasia and degeneration in *rd7/rd7* mice. *Hum. Mol. Genet.* **10**, 1619–1626 (2001).
14. Kosaka, J., Suzuki, A., Morii, E. & Nomura, S. Differential localization and expression of α and β isoenzymes of protein kinase C in the rat retina. *J. Neurosci. Res.* **54**, 655–663 (1998).
15. Saari, J.C. *et al*. Cellular retinaldehyde-binding protein is expressed by oligodendrocytes in optic nerve and brain. *Glia* **21**, 259–268 (1997).
16. Zhao, X., Huang, J., Khani, S.C. & Palczewski, K. Molecular forms of human rhodopsin kinase (GRK1). *J. Biol. Chem.* **273**, 5124–5131 (1998).
17. Verderber, L., Johnson, W., Mucke, L. & Sarthy, V. Differential regulation of a glial fibrillary acidic protein-LacZ transgene in retinal astrocytes and Muller cells. *Invest. Ophthalmol. Vis. Sci.* **36**, 1137–1143 (1995).
18. Fan, W., Lin, N., Sheedlo, H.J. & Turner, J.E. Müller and RPE cell response to photoreceptor cell degeneration in aging Fischer rats. *Exp. Eye. Res.* **63**, 9–18 (1996).
19. Williams, D.S. Actin filaments and photoreceptor membrane turnover. *BioEssays* **13**, 171–178 (1991).
20. Cepko, C.L., Austin, C.P., Yang, X., Alexiades, M. & Ezzeddine, D. Cell fate determination in the vertebrate retina. *Proc. Natl Acad. Sci. USA* **93**, 589–595 (1996).
21. Cepko, C.L. The roles of intrinsic and extrinsic cues and bHLH genes in the determination of retinal cell fates. *Curr. Opin. Neurobiol.* **9**, 37–46 (1999).
22. Livesey, F.J. & Cepko, C.L. Vertebrate neural cell-fate determination: lessons from the retina. *Nature Rev. Neurosci.* **2**, 109–118 (2001).
23. Harris, W.A. & Messersmith, S.L. Two cellular inductions involved in photoreceptor determination in the *Xenopus* retina. *Neuron* **9**, 357–372 (1992).
24. Tybulewicz, V.L.J., Crawford, C.E., Jackson, P.K., Bronson, P.T. & Mulligan, R.C. Neonatal lethality and lymphopenia in mice with a homozygous disruption of the c-abl proto-oncogene. *Cell* **65**, 1153–1163 (1991).
25. Nagy, A., Rossant, J., Nagy, R., Abramow-Newerly, W. & Roder, J.C. Derivation of completely cell culture-derived mice from early-passage embryonic stem cells. *Proc. Natl Acad. Sci. USA* **90**, 8424–8428 (1993).
26. Kendall, S.K., Samuelson, L.C., Saunders, T.L., Wood, R.I. & Camper, S.A. Targeted disruption of the pituitary glycoprotein hormone α-subunit produces hypogonadal and hypothyroid mice. *Genes Dev.* **9**, 2007–2019 (1995).
27. Hitchcock, P.F. Morphology and distribution of synapses onto a type of large field ganglion cell in the retina of the goldfish. *J. Comp. Neurol.* **283**, 177–188 (1989).
28. Sambrook, J. & Russell, D.W. *Molecular Cloning: A Laboratory Manual* 3rd edn. (Cold Spring Harbor Laboratory Press, Cold Spring Harbor, New York, 2001).
29. Coligan, J.E., Dunn, B.M., Ploegh, H.L., Speicher, D.W. & Wingfield, P.T. *Current Protocols in Protein Science* (John Wiley and Sons, 1999).
30. Toda, K., Bush, R.A., Humphries, P. & Sieving, P.A. The electroretinogram of the rhodopsin knock-out mouse. *Vis. Neurosci.* **16**, 391–398 (1999).
31. Ng, L. *et al*. A thyroid hormone receptor that is required for the development of green cone photoreceptors. *Nature Genet.* **27**, 94–98 (2001).